

## **Inhibitive Effect of Azorubine Dye on the Corrosion of Mild Steel in Hydrochloric Acid Medium and Synergistic Iodide Additive**

*Sudhish K. Shukla, Ashish K. Singh, Lutendo C. Murulana, Mwadham M. Kabanda and Eno E. Ebenso\**

Department of Chemistry, School of Mathematical and Physical Sciences, North West University (Mafikeng Campus), Private Bag X2046, Mmabatho 2735, South Africa.

\*E-mail: [Eno.Ebenso@nwu.ac.za](mailto:Eno.Ebenso@nwu.ac.za)

*Received: 24 April 2012 / Accepted: 16 May 2012 / Published: 1 June 2012*

---

The inhibition performance of Azorubine dye (AZB) on mild steel corrosion in hydrochloric acid solution was studied at 303-333K using weight loss and hydrogen evolution techniques. The effect of inhibitor concentration on inhibition efficiency has been studied. Inhibition efficiency increased and corrosion rate decreased with increase in concentration of AZB. The adsorption of AZB on mild steel obeyed the Langmuir adsorption isotherm model. Physical adsorption is proposed from the values of  $E_a$  and  $\Delta G_{ads}$  obtained. Synergism parameter evaluated was found to be greater than unity for all concentrations of AZB suggesting that the increase in the inhibition efficiency of inhibitor by the addition of halide ion is only due to the synergism.

---

**Keywords:** Mild steel; Corrosion inhibition; Dye, Weight loss study; Adsorption

### **1. INTRODUCTION**

Steel is the most important engineering and construction material in the world. It is used in every aspect of our lives [1]. There are the various types of steels reported to be used in the different applications. Mild steel is one of the most used steel types in industries. Organic compounds having hetero atoms such as nitrogen, sulphur, oxygen, have been reported as good corrosion inhibitors [1-8]. Inhibition efficiency depends upon the adsorption ability of the inhibitor molecule and the stability of the adsorbed layer which acts as a barrier to separate the metal surface from the corroding medium [9-11]. The adsorption of the inhibitor molecules depends upon the nature of the functional group adsorbed on the metal surface.

In recent years, attention has been focused on the investigation of organic dyes as potential inhibitors for the metals in corrosive environment [12-20]. Most of the dyes consist of double bonds, hetero atoms and aromatic rings. All these functional groups present in the molecules which leads towards the dyes being considered good corrosion inhibitors.

In present study, Azorubine dye (AZB) was used as corrosion inhibitor. It is a synthetic red food dye from the azo dye group. Its chemical name is, disodium 4- hydroxy-2- [(E)-(4-sulfonato-1-naphthyl) diazonyl] naphthalene-1-sulfonate. The molecular structure of the Azorubine is given in figure1. The azo and sulphonate groups and electron cloud on the aromatic ring suggest that AZB should act as a good corrosion inhibitor.

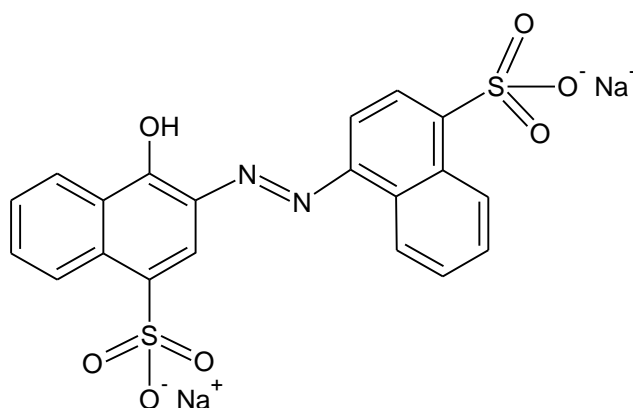


**Figure 1.** Structure of Azorubine dye (AZB)

## 2. EXPERIMENTAL

The mild steel used in the study had the following composition (wt %), C (0.19), Si (0.26), Mn (0.64), S (0.05), P (0.06), Ni (0.09), Cr (0.08), Mo (0.02), Cu (0.27), and the remainder iron (Fe). The mild steel coupons were prepared, degreased and cleaned as previously reported [20]. The concentration of the blank corrodent, HCl (BDH Chemical Supplies Laboratory, England) prepared and used was 1M. Azorubine dye (AZB) (an azo dye) [disodium 4- hydroxy-2- [(E)-(4-sulfonato-1-naphthyl) diazonyl] naphthalene-1-sulfonate used, as inhibitor in the present study is a product of Merck Chemicals, UK. A stock solution of AZB (0.005M) was prepared by weighing an appropriate amount of it and dissolved in 1 litre of 1M HCl. Other concentrations (0.0001 – 0.01M) were obtained from the stock solution following serial dilution. The halide salt (KI) used was obtained from BDH Laboratory Supplies, England. Similarly, a stock solution of 0.1M was prepared by weighing an appropriate amount of the halide salt and dissolved in 1 litre of 1M HCl. However, 0.05M KI was used for the synergistic study. All preparations were carried out using deionized water. All chemicals and reagents used were of analytical grade. They were used as sourced without further preparation.

The apparatus and procedure followed for weight loss and hydrogen evolution methods were similar to that earlier reported [20]. In the weight loss method, the progress of the corrosion reaction was monitored by determining the weight loss of the coupons (obtained as the differences in the weight of the coupons after immersion in different solutions of the system and the original weight of

the coupons) and careful measurement of the volume of hydrogen gas evolved for weight loss and hydrogen evolution methods respectively at fixed time intervals. In both techniques, the experiments were conducted at 303 to 333K maintained in a thermostatic bath.

### 3. RESULTS AND DISCUSSION

#### 3.1. Hydrogen evolution technique:

Hydrogen evolution technique is one of the methods used to study the inhibitive property of AZB. The values calculated from the hydrogen evolution data are presented in table 1. The graphs of inhibition efficiency and corrosion rate against inhibitor concentration are shown in figures 2 and 3 respectively. It is evident from the figures that the inhibition efficiency increases with increase in the inhibitor concentration. It is evident from the table 1 that the corrosion rate decreases and inhibition efficiency increases with increase in the inhibitor concentration. Increase in the inhibition efficiency suggests that AZB molecule exhibits good interaction with the metal surface.

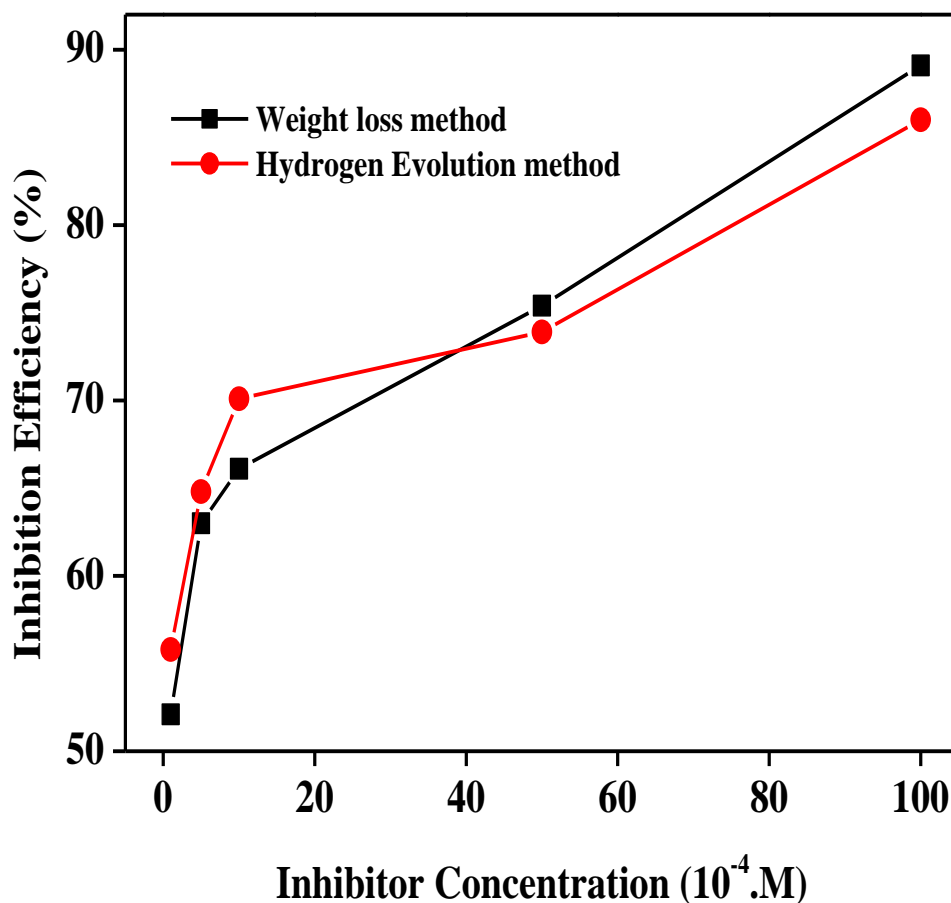


**Figure 2.** Plot of inhibition efficiency against inhibitor concentration for mild steel corrosion in 1M hydrochloric acid solution at 303K.

**Table1.** Weight loss and hydrogen evolution data for the mild steel corrosion in the presence and absence of the different concentration of AZB in 1M HCl at 303 K.

| Inhibitor conc. $\times 10^{-4}$ M | Weight Loss data |                      |          | Hydrogen evolution data |                      |          |
|------------------------------------|------------------|----------------------|----------|-------------------------|----------------------|----------|
|                                    | IE (%)           | Corrosion Rate (mpy) | $\theta$ | IE (%)                  | Corrosion Rate (mpy) | $\theta$ |
| Blank                              | -                | 110.4                | -        | -                       | 39.4                 | -        |
| 1                                  | 52.1             | 51.0                 | 0.52     | 55.8                    | 17.4                 | 0.56     |
| 5                                  | 63.0             | 40.1                 | 0.63     | 64.8                    | 14.0                 | 0.65     |
| 10                                 | 66.1             | 37.2                 | 0.66     | 70.1                    | 12.0                 | 0.70     |
| 50                                 | 75.4             | 27.0                 | 0.75     | 73.9                    | 11.2                 | 0.74     |
| 100                                | 89.1             | 12.0                 | 0.89     | 86.0                    | 6.1                  | 0.86     |

3.2. Weight loss technique:

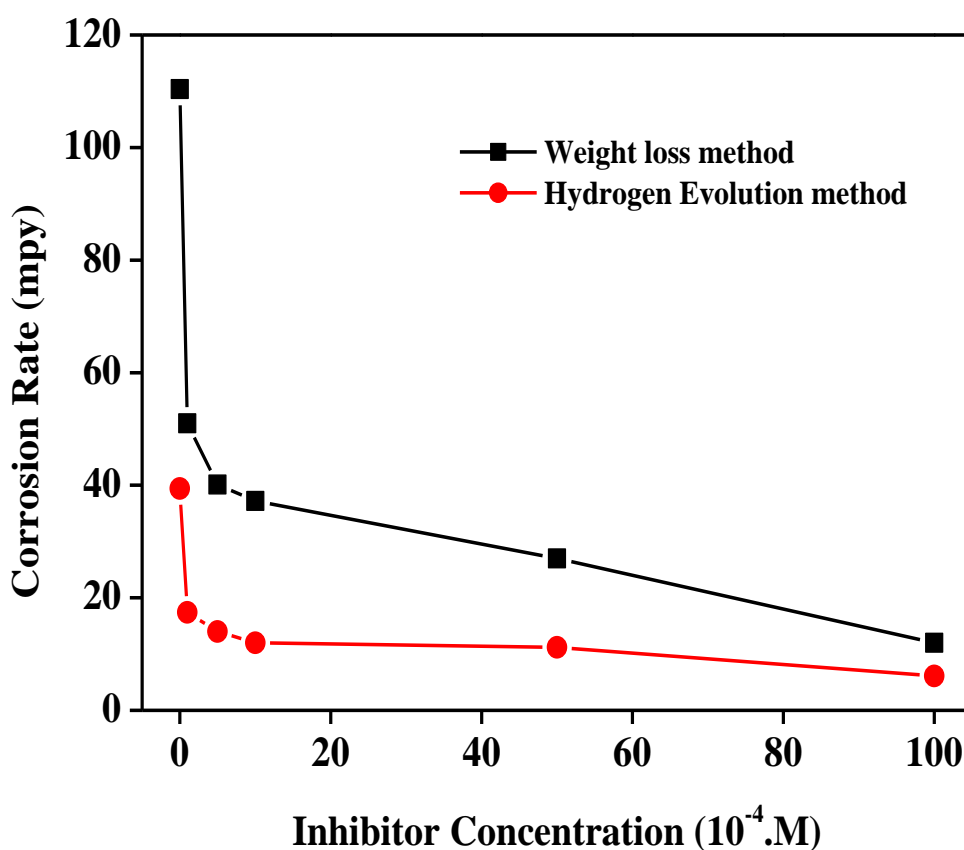


**Figure 3.** Plot of corrosion rate against inhibitor concentration for mild steel corrosion in 1M hydrochloric acid solution at 303K.

The values of % inhibition efficiency and corrosion rate calculated from the weight loss method at different concentrations of AZB in 1M HCl at 303 K are also presented in table1. The variation in inhibition efficiency and corrosion rate with the inhibitor efficiency can also be seen in figure 2 and 3 respectively. It was observed from Table 1 that AZB inhibits the mild steel corrosion in

1M HCl at all the concentrations used in study. Maximum inhibition efficiency was shown at  $100 \times 10^{-4}$  M concentration of AZB. It is evident that the corrosion rate decreased with increase in the inhibition efficiency. Results obtained from the weight loss studies are in good agreement with the hydrogen evolution technique.

### 3.3. Adsorption isotherm

Adsorption of the inhibitor molecules mainly dependent on the charge and the nature of the metal surface, electronic characteristics of the metal surface, temperature, adsorption of the solvent, ionic species and the electrochemical potential at the solution interface. The adsorption isotherm describes the adsorptive behavior of organic compounds in order to know the adsorption mechanism. The most frequently used adsorption isotherms are Langmuir, Temkin, Frumkin and Freundlich isotherm. To obtain the adsorption isotherm, the degree of surface coverage ( $\theta$ ) was calculated for various concentrations of the AZB from the weight loss data and listed in Table 1.

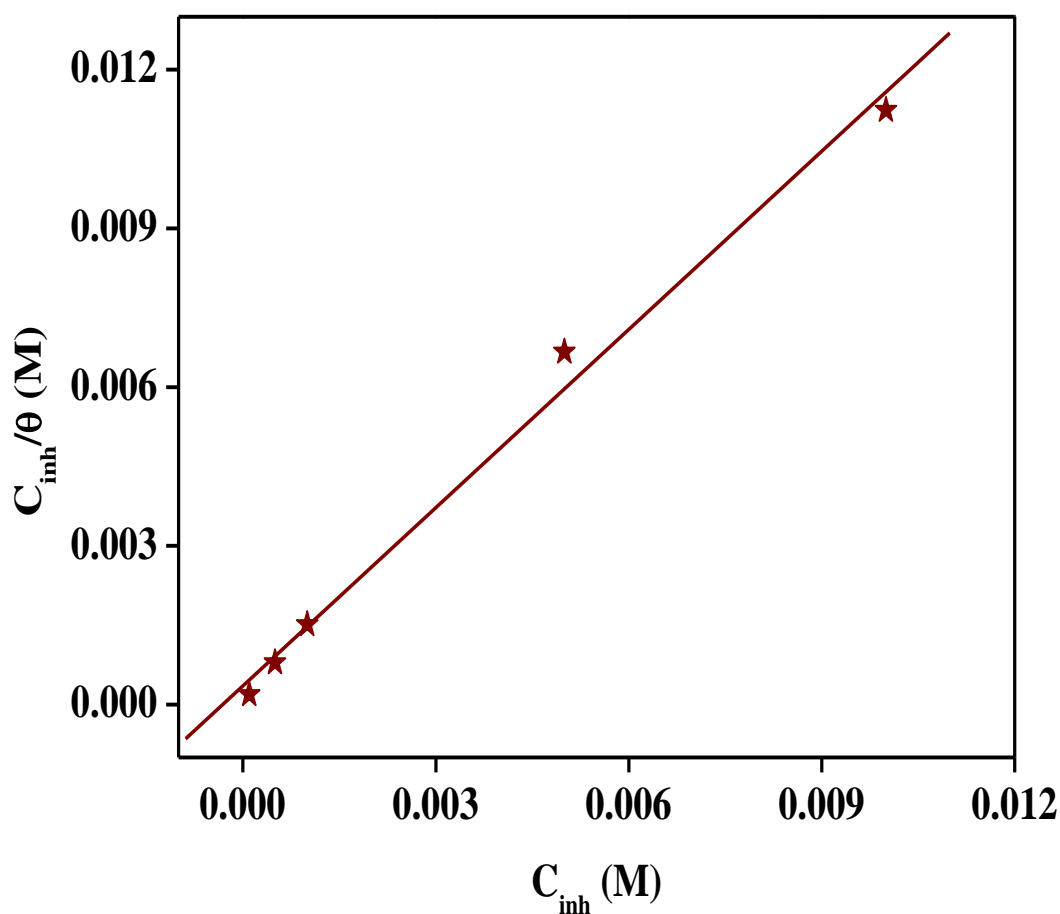


**Figure 4.** Langmuir adsorption isotherm for the mild steel corrosion in the presence of AZB at 303 K.

Langmuir adsorption isotherm was tested to its fit with the experimental data. Langmuir adsorption isotherm is represented by the equation:

$$\frac{C_{inh}}{\theta} = \frac{1}{K_{ads}} + C_{inh} \quad (1)$$

where,  $K_{ads}$  is the adsorption equilibrium constant,  $\theta$  is the degree of surface coverage and  $C_{inh}$  is molar concentration of the inhibitor used. A straight line was obtained by plotting the graph of  $C_{inh}/\theta$  vs  $C_{inh}$  for AZB and the regression coefficient obtain was almost unity (Figure 4). This result suggests that the Langmuir adsorption isotherm gives the best description of the adsorption behavior of the AZB on the metal surface. The parameters calculated from the adsorption isotherm were listed in Table 2.

**Table 2.** Langmuir adsorption isotherm parameters

| Temp (K) | $K_{ads}$ ( $\text{mol}^{-1}$ ) | Slope   | $R^2$   | $\Delta G_{ads}$ ( $\text{kJ mol}^{-1}$ ) |
|----------|---------------------------------|---------|---------|---|
| 303      | $2.832 \times 10^3$             | 1.12278 | 0.99612 | -30.15                                    |

### 3.4. Effect of temperature: Kinetic and Thermodynamic consideration

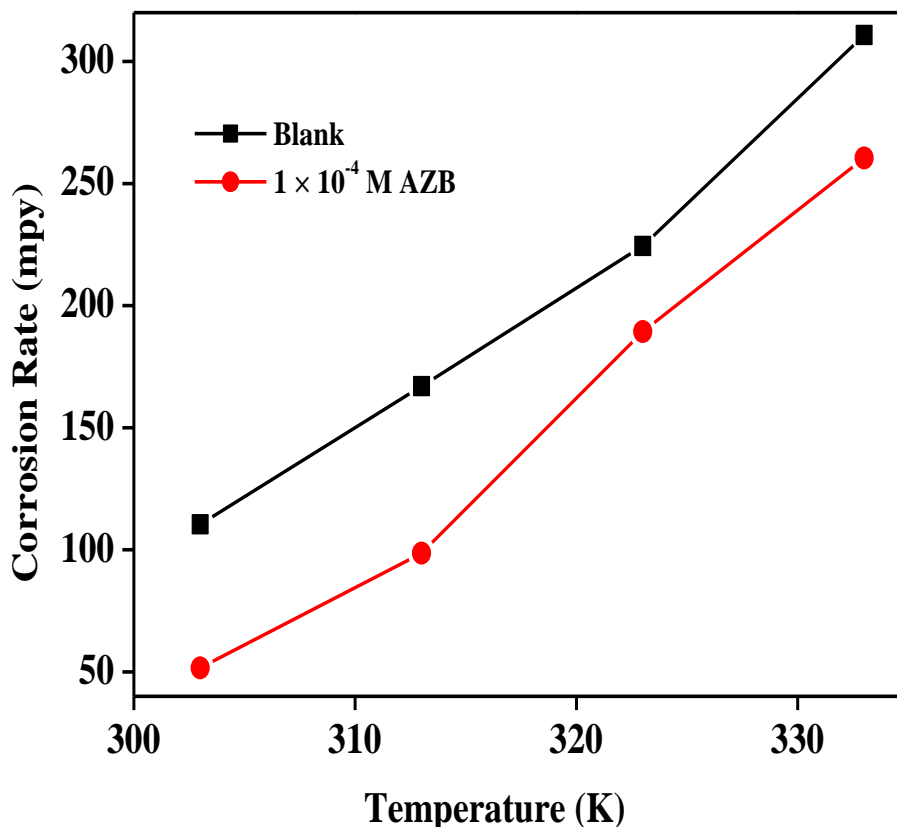


**Figure 5.** Effect of temperature on corrosion rate with and without  $1 \times 10^{-4}$  M AZB

The increase in the temperature resulted in the increase in the corrosion rate for both inhibited and uninhibited system. The increase in the corrosion rate without inhibitor is higher than the inhibited

system. Decrease in the corrosion rate with temperature (303K-333K) by addition of AZB is shown in figure5.

It is well known that the logarithm of the corrosion rate is a linear function with 1/T i.e. Arrhenius equation [21-22]:

$$\log C_r = \frac{-E_a}{2.303RT} + \log \lambda \tag{2}$$

where,  $E_a$  is the apparent effective activation energy, R molar gas constant and  $\lambda$  the Arrhenius pre exponential factor.

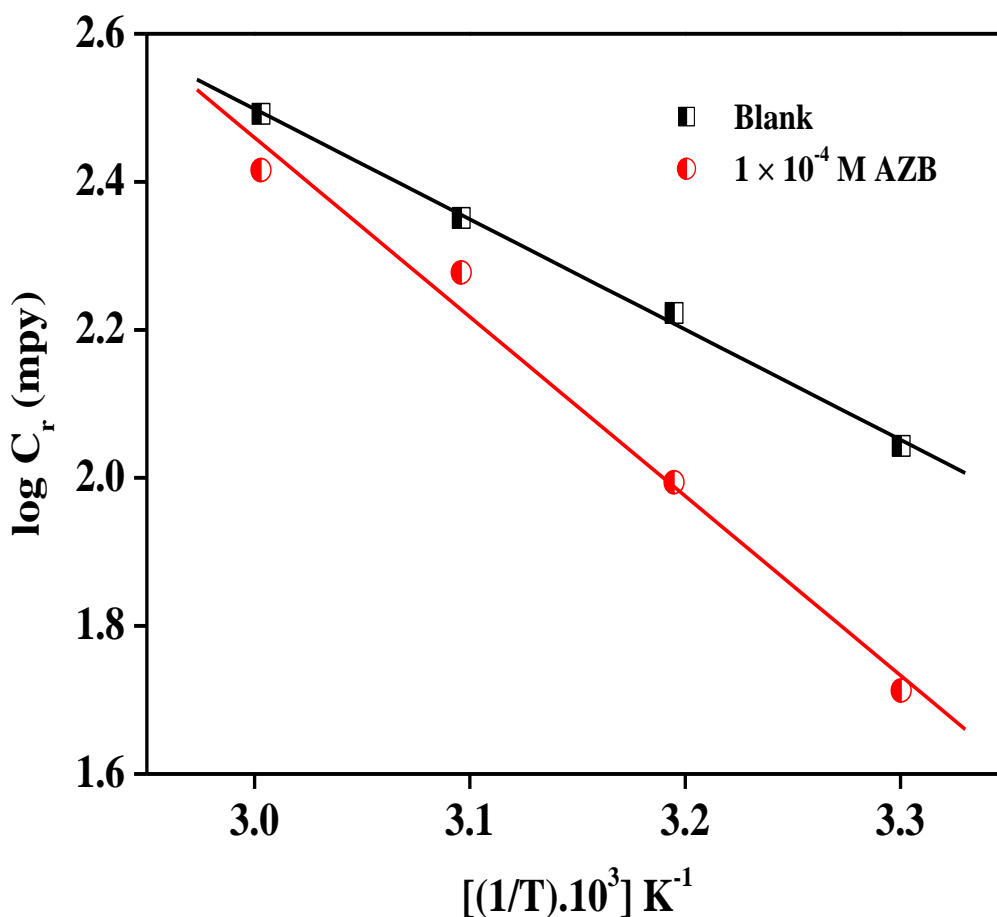


**Figure 6.** Arrhenius plot for mild steel corrosion in 1M HCl in the absence and presence of  $1 \times 10^{-4}$  M AZB

A plot of log of corrosion rate obtained from the weight loss study against 1/T gave straight line, as shown in figure 6. The apparent activation energy obtained from the slope ( $-E_a / 2.303R$ ) of the lines and the pre exponential factor obtained from the intercept are given in Table 3. It is clear from Table 3 that the apparent activation energy value increased on addition of AZB in comparison to the uninhibited solution. Increase in the apparent activation energy is interpreted as the physical adsorption of the inhibitor molecule on the mild steel surface. The increase in the activation energy is attributed to

an appreciable decrease in the adsorption of the inhibitor on mild steel surface with increase in the temperature. This leads to the increase in the corrosion rate due to the greater area of metal surface being exposed towards the acidic environment [23]. The decrease in the corrosion rate by increasing the inhibitor concentration suggests that the apparent activation energy ( $E_a$ ) is the deciding factor rather than the pre exponential factor ( $\lambda$ ).

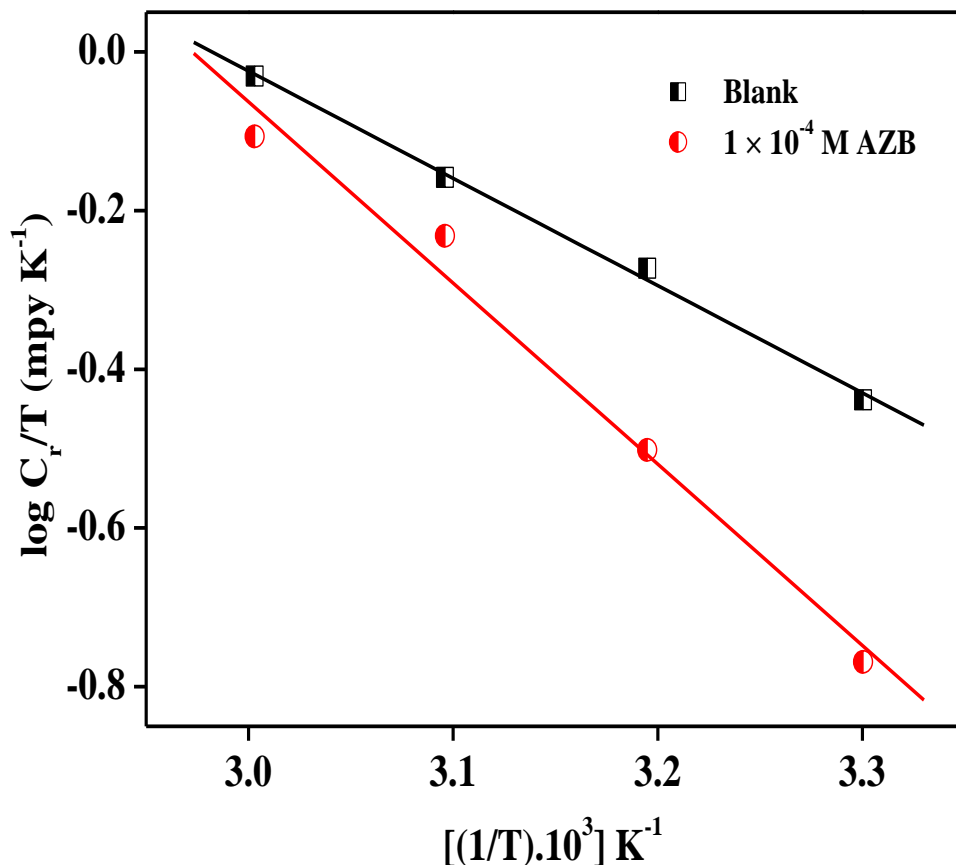


**Figure 7.** Transition state plot for mild steel corrosion in 1M HCl in absence and presence of  $1 \times 10^{-4}$  M AZB

Dependence of the corrosion rate on temperature is also expressed using the Arrhenius equation of the transition state [24]:

$$C_R = \frac{RT}{NH} \exp\left(\frac{\Delta S^*}{R}\right) \exp\left(-\frac{\Delta H^*}{RT}\right) \tag{3}$$

where,  $h$  is Plank’s constant,  $N$  the Avogadro’s number,  $\Delta S^*$  the apparent entropy of activation and  $\Delta H^*$  the enthalpy of activation. A plot of  $\log (C_R/T)$  versus  $1/T$  is shown in Figure7. Straight lines were obtained with slope  $(-\Delta H^*/2.303R)$  and an intercept of  $[\log(R/Nh) + (\Delta S^*/2.303R)]$ , from which  $\Delta H^*$  and  $\Delta S^*$  were calculated and listed in Table 3. It is clear from Table 3, that entropy of activation ( $\Delta S^*$ ) increased in the presence of inhibitor compared to the uninhibited sample. The

increase in the activation entropy in the presence of inhibitor indicates increase in the disorderliness on going from reactant to activated complex. It is evident from the table that the value of  $\Delta H^*$  increases with the presence of inhibitor than the uninhibited solution indicating higher inhibitive efficiency. This may be attributed to the presence of an energy barrier for the reaction, hence, the process of adsorption of inhibitor leads to rise in enthalpy of the corrosion process.

**Table 3.** Kinetic/thermodynamic parameters for mild steel corrosion in 1M HCl.

| Inhibitor conc.<br>( $\times 10^{-4}$ M) | Ea<br>(kJ mol <sup>-1</sup> ) | $\lambda$<br>(mg cm <sup>-2</sup> ) | $\Delta H^*$<br>(kJ mol <sup>-1</sup> ) | $\Delta S^*$<br>(J mol <sup>-1</sup> K <sup>-1</sup> ) |
|--|-------------------------------|-------------------------------------|---|--|
| Blank                                    | 28.53                         | 9.3 $\times 10^6$                   | 25.89                                   | -120.20  |
| 1.0                                      | 46.38                         | 5.3 $\times 10^9$                   | 43.74                                   | -67.41   |

Free energy of adsorption ( $\Delta G_{ads}$ ) was calculated using the following equation [25]:

$$K_{ads} = \frac{1}{55.5} \exp \left[ \frac{-\Delta G_{ads}^0}{RT} \right] \quad (4)$$

This equation can also be express in the form as follows:

$$\Delta G_{ads} = -2.303 RT \log(55.5K_{ads}) \quad (5)$$

where,  $\Delta G_{ads}$  is Gibbs free energy of adsorption, T is the temperature in Kelvin and  $K_{ads}$  is the equilibrium constant for the adsorption process and 55.5 is the molar concentration of water in solution.  $K_{ads}$  value was calculated from the intercept of Figure 4 and presented in Table 2.  $\Delta G_{ads}$  values calculated from eq. 5 is also listed in Table 2. The negative value of Gibbs free energy ensures the spontaneity of adsorption process and stability of the adsorbed layer on the surface of mild steel.

#### 3.4. Effect of KI on the inhibition efficiency: Synergistic effect

It is accepted that the presence of halide ions in acidic medium synergistically increases the inhibition efficiency of some organic compounds. It is assumed that the role of halide ions is to improve the adsorption of the organic cations by forming intermediate bridge between positively charged metal surface and the positive end of the inhibitor [20]. According to Oguzie *et al.* (2007) [26] synergism results from the increase in the surface coverage by the ion-pair interaction between organic cation and anion. Synergistic ability of the halide ion increases in order  $Cl^- < Br^- < I^-$  [2]. The greater influence of the iodide ion is attributed to be due to the larger ionic radius, low electro negativity and high hydrophobicity as compared to the other halides [27].

**Table 4.** Weight loss data in the presence of KI with and without AZB on mild steel corrosion in 1M HCl at 303 K and the synergism parameters

| Inhibitor concentration              | IE (%) | $\theta$ | Synergism parameter ( $S_1$ ) |
|--------------------------------------|--------|----------|-------------------------------|
| Blank                                | -      | -        | -                             |
| 0.05 M KI                            | 32     | 0.32     | -                             |
| $1 \times 10^{-4}$ M AZB + 0.05 M KI | 70.2   | 0.70     | 1.20                          |
| $5 \times 10^{-4}$ M AZB + 0.05 M KI | 73.4   | 0.73     | 1.30                          |
| $1 \times 10^{-3}$ M AZB + 0.05 M KI | 80.2   | 0.80     | 1.23                          |
| $5 \times 10^{-3}$ M AZB + 0.05 M KI | 90.1   | 0.90     | 1.19                          |
| $1 \times 10^{-2}$ M AZB + 0.05 M KI | 96.4   | 0.96     | 1.26                          |

Inhibition efficiency of the different concentrations of AZB with the 0.05 M KI is presented in Table 4. The graph plotted between inhibition efficiency and inhibitor concentration in the presence of KI is shown in figure 8. Comparison of inhibition efficiency with the KI reported in Table 4 and without KI reported in Table 1, concludes that the addition of KI shows synergistic effect with the AZB.

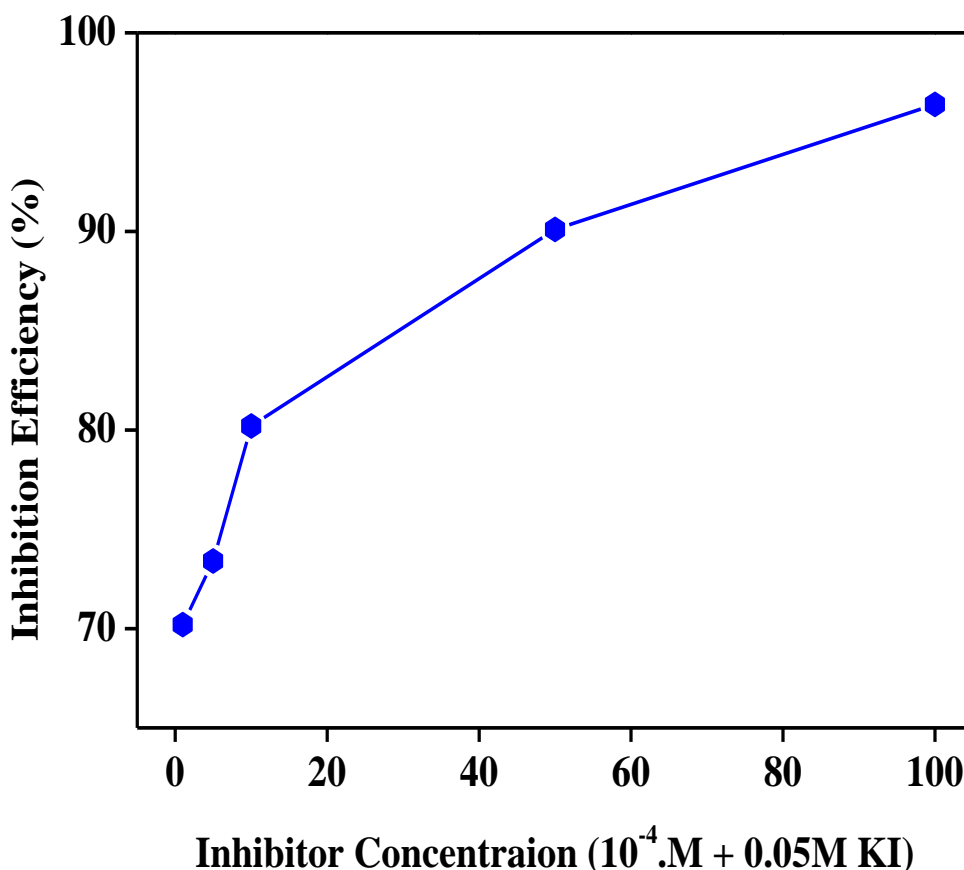


**Figure 8.** Plot of inhibition efficiency against various concentration of AZB + 0.05M KI for mild steel corrosion in 1M hydrochloric acid solution at 303K.

The synergistic parameter  $S_1$ , was evaluated using the relationship given by Aramaki and Hackerman [27, 28]:

$$S_1 = \frac{1 - I_{1+2}}{1 - I'_{1+2}} \quad (6)$$

where,  $I_{1+2} = (I_1 + I_2)$ ,  $I_1$  = inhibition efficiency of the iodide,  $I_2$  = inhibition efficiency of AZB,  $I'_{1+2}$  = measured inhibition efficiency of AZB in combination with iodide ion. This parameter was obtained from the inhibition efficiency values obtained from the weight loss data.  $S_1$  values calculate from the eq 6 is presented in Table4. It is clear from the data that the  $S_1$  values are greater than unity. This indicates that the improvement in the inhibition efficiency by the addition of iodide ion is due to the synergistic effect. Feng *et al.* (1999) and Durnie *et al.* (1999) [29, 30] also reported the similar results. The synergistic effect of KI with AZB is due to the stabilization of inhibitor molecule on to the mild steel surface. This stabilization may be attributed to the interaction between AZB and I<sup>-</sup> ions. This interaction enhances the inhibition efficiency due to the increase in the surface coverage.

#### 4. CONCLUSIONS

1. Results obtained from the two techniques studied shows that AZB acts as an effective inhibitor for the corrosion of mild steel in HCl solution.
2. Increase in the inhibitor concentration decreased the corrosion rate whereas increase in the temperature causes increase in the corrosion rate.
3. The adsorption of AZB follows the Langmuir adsorption isotherm model.
4. Synergistic effect was observed between AZB and KI.
5. Phenomenon of the physical adsorption is proposed on the basis of kinetic and thermodynamic parameters.

#### ACKNOWLEDGEMENTS

SKS, AKS and MMK thank the North-West University for Postdoctoral Fellowship. EEE acknowledges the National Research Foundation (NRF) of South Africa for funding.

#### References

1. S.S.A. El-Maksoud, *Int. J. Electrochem. Sci.*, 3 (2008) 528.
2. S.A. Umoren, I.B. Obot, E.E. Ebenso, *E-Journal of Chemistry*, 5 (2008) 355.
3. S.K. Shukla, M.A. Quraishi, *Corros. Sci.*, 51 (2009) 1007.
4. S.K. Shukla, M.A. Quraishi, *Corros. Sci.*, 52 (2010) 314.
5. I.B. Obot, N.O. Obi-Egbedi, S.A. Umoren, E.E. Ebenso, *Int. J. Electrochem. Sci.*, 5 (2010) 994.
6. F.Bentiss, M. Lebrini, M. Traisnel, M. Lagrenee, *J. Appl. Electrochem.*, 39 (2009) 1399.
7. M.A. Quraishi, I. Ahmad, A.K. Singh, S.K. Shukla, B. Lal, V. Singh, *Mater. Chem. Phys.*, 112 (2008) 1035.

8. S.K. Shukla, M.A. Quraishi, R. Prakash, *Corros. Sci.*, 50 (2008) 2867.
9. H. Keles, M. Keles, I. Dehri, O. Serindag, *Mater. Chem. Phys.*, 112(2008) 173.
10. S. Vishwanatham, N. Halidar, *Corros. Sci.*, 50 (2008) 2999.
11. M.A. Quraishi, S.K. Shukla, *Mater. Chem. Phys.*, 113 (2009) 685.
12. E.E. Oguzie, E.E. Ebenso, *Pigment & Resin Technol.*, 35 (2006) 30.
13. E.E. Ebenso, E.E. Oguzie, *Mater. Letts.* 59 (2005) 2163.
14. E.E. Ebenso, *Niger. Jour. Chem. Res.*, 6 (2001) 8.
15. E.E. Ebenso, *Bull. Electrochem.* 19 (2003) 209.
16. E.E. Ebenso, *Bull. Electrochem.* 20 (2005) 551.
17. L. Tang, G. Mu, G. Liu, *Corros. Sci.*, 45 (2003) 2251.
18. L. Tang, X. Li, G. Mu, G. Liu, *Appl. Surf. Sci.*, 252 (2006) 6394.
19. H.A. Sorkhabi, B. Masoumi, P. Ejbari, E. Asghari, *J. Appl. Electrochem.*, 39 (2009) 1497.
20. E.E. Ebenso, H. Alemu, S.A. Umoren, I.B. Obot, *Int. J. Electrochem. Sci.*, 3 (2008) 1325.
21. C.B. Breslin, W.M. Carroll, *Corros. Sci.*, 34 (1993) 327.
22. M.G.A. Khedr, M.S. Lashien, *Corros. Sci.*, 33 (1992) 137.
23. T.Szauer, A. Brandt, *Electrochim. Acta*, 26 (1981) 1253.
24. S.S.A. El Rehim, H.H. Hassan, M.A. Amin, *Mater. Chem. Phys.*, 70 (2001) 64.
25. M. Schorr, J. Yahalom, *Corros. Sci.*, 12 (1972) 867.
26. E.E. Oguzie, Y. Li, F.H. Wang, *Colloid and Interface Sci.*, 310 (2007) 90.
27. S.A. Umoren, E.E. Ebenso, *Mater. Chem. Phys.*, 106 (2007) 387.
28. S.A. Umoren, E.E. Ebenso, O. Ogbobe, *J. Appl. Polym. Sci.*, 113 (2009) 3533.
29. Y. Feng, K.S. Siow, W.K. Teo, A.K. Hsieh, *Corros. Sci.*, 41 (1999) 829.
30. W. Durnie, R.D. Marco, A. Jefferson, B. Kinsella, *J. Electrochem. Soc.*, 14 (1999) 1751.